Matrix Biology Plus 23 (2024) 100154

Contents lists available at ScienceDirect

Matrix Biology Plus

journal homepage: www.sciencedirect.com/journal/matrix-biology-plus

Topographic modification of the extracellular matrix precedes the onset of bladder cancer

Chiara Venegoni [a], Filippo Pederzoli [a,b], Irene Locatelli [a], Elisa Alchera [a], Laura Martinez-Vidal [a,b], Alessia Di Coste [a], Marco Bandini [a,b], Andrea Necchi [a,b], Francesco Montorsi [a,b], Andrea Salonia [a,b], Marco Moschini [a,b], Jithin Jose [c], Federico Scarfò [d], Roberta Lucianò [d], Massimo Alfano [a,*]

[a] Division of Experimental Oncology/Unit of Urology, URI, IRCCS Ospedale San Raffaele, Milan, Italy
[b] Università Vita-Salute San Raffaele, Milan, Italy
[c] FUJIFILM Visualsonics Inc., Amsterdam, the Netherlands
[d] Pathology Unit, IRCCS Ospedale San Raffaele, Milan, Italy

ARTICLE INFO

Keywords:
Anisotropy
Bladder
Cancer
Carcinogen
Collagen
Extracellular matrix
Radiotherapy

ABSTRACT

Background: Non-muscle invasive bladder cancer (NMIBC) patients are affected by a high risk of recurrence. The topography of collagen fibers represents a hallmark of the neoplastic extracellular microenvironment.
Objective: Assess the topographic change associated with different stages of bladder cancer (from neoplastic lesions to *bona fide* tumor) and whether those changes favour the development of NMIBC.
Design, Setting, and Participants: Seventy-one clinical samples of urothelial carcinoma at different stages were used. Topographic changes preceding tumor onset and progression were evaluated in the rat bladder cancer model induced by nitrosamine (BBN), a bladder-specific carcinogen. The preclinical model of actinic cystitis was also used in combination with BBN. Validated hematoxylin-eosin sections were used to assess the topography of collagen fibrils associated with pre-tumoral steps, NMIBC, and MIBC.
Findings: Linearization of collagen fibers was higher in Cis and Ta vs. dysplastic urothelium, further increased in T1 and greatest in T2 tumors. In the BBN preclinical model, an increase in the linearization of collagen fibers was established since the beginning of inflammation, such as the onset of atypia of a non-univocal nature and dysplasia, and further increased in the presence of the tumor. Linearization of collagen fibers in the model of actinic cystitis was associated with earlier onset of BBN-induced tumor.
Conclusions: The topographic modification of the extracellular microenvironment occurs during the inflammatory processes preceding and favoring the onset of bladder cancer. The topographic reconfiguration of the stroma could represent a marker for identifying and treating the non-neoplastic tissue susceptible to tumor recurrence.

Introduction

Physical and mechanical properties of the extracellular matrix (ECM) are fundamental to determining cell phenotypes both in healthy and pathological conditions [1–7]. ECM remodeling in the tumor microenvironment (TME) influences cancer cell survival and spreading, immune cells anticancer activity, and interaction of cancer-associated fibroblasts with cancer cells [8,9]. Among the different ECM properties, ECM anisotropy – the topographical alignment of the ECM collagen fibers [3,10] is an emerging prognostic factor in tumors. Indeed, the highly aligned fibers in the TME influence gene expression, differentiation, proliferation, and migration of cancer cells while serving as physical tracks for tumor invasion and spreading [2,11,12]. Linearization of the texture of collagen fibers, modification of the biochemical composition of the TME, and increased level of the extracellular lysyl oxidase (LOX) have been associated with increased tissue stiffness in ovarian, colorectal and breast cancer and Hodgkin lymphomas, generally resulting in an unfavorable prognostic factor for affected patients [1,4,6,13,14]. Noteworthy, the altered organization of collagen fibers has also been reported in the perilesional tissue, such as human colon mucosa up to twenty centimeters far from the tumor [2,3], and demonstrated to support proliferation and invasion of tumor cells[15].

* Corresponding author at: Urological Research Institute (URI), DiBit2, Scientific Institute San Raffaele, Via Olgettina, 60, 20132 Milan, Italy.
E-mail address: alfano.massimo@hsr.it (M. Alfano).

https://doi.org/10.1016/j.mbplus.2024.100154
Received 29 April 2024; Received in revised form 28 May 2024; Accepted 31 May 2024
Available online 2 June 2024

In bladder cancer (BCa), increased linearization of collagen fibers has been reported in the neoplastic tissue from patients with muscle-invasive bladder cancer (MIBC) [16], while the topographical reorganization of the ECM in the TME remains undefined in non-muscle invasive bladder cancer (NMIBC). As NMIBC is characterized by a very high frequency of relapse that is still difficult to predict using traditional histology parameters, ECM remodeling in the TME represents an emerging and promising biomarker of cancer recurrence [17]. In this study, we aimed to establish the topography of collagen fibers in the whole spectrum of bladder cancer progression – from in non-neoplastic and dysplastic tissues to *bona fide* bladder cancer – and its association with tumor grades and stages, leveraging tissue specimens from patients and relevant bladder cancer rat models. Second, a combination of rodent models was used to establish whether topographic modification occurring during dysplasia sustains the onset of bladder cancer.

Results

Standardization of the anisotropy measurement in human histological sections

The topographic reconfiguration of the stroma was assessed through the linearization assessment of the collagen fibers pattern (anisotropy index). To identify the area of the tissue representative of the anisotropy index of the entire histological section, the protocol for measuring the anisotropy index was standardized using human bladder tissues from 10 therapy-naïve patients undergoing radical cystectomy (Table 1).

Table 1
Characteristics of patients with urothelial carcinoma.

TURBT pre-BCG					
#	Stage	Grade	Sex	Age (Y)	Smoke
1	T1	G3	M	65	Ex
2	T1	G3	M	84	Ex
3	T1	G3	M	56	No
4	T1	G3	M	57	No
5	T1	G3	M	68	Yes
6	T1	G3	M	69	Ex
7	Ta	G2	M	63	Ex
8	Ta	G2	M	67	No
9	Ta	G3	M	67	Ex
10	Cis	G3	M	58	Yes
11	T1	G3	M	81	Yes
12	T1	G3	M	74	Ex
13	T1	G3	M	83	Yes
14	Ta	G3	M	69	No
15	Ta	G3	M	44	No
16	Cis	G3	M	54	No
17	Ta, Cis	G3	M	70	Ex
18	Ta	G2	F	62	No
19	Ta	G2	F	69	No
20	Ta	G2	M	72	Ex
Therapy naïve –radical cystectomy					
#	Stage	Grade	Sex	Age (Y)	Smoke
21	T2b	G3	M	69	Ex
22	T3b	G3	F	70	No
23	T3b	G3	M	76	No
24	T3a	G3	M	77	Ex
25	T2b	G3	M	62	No
26	T2b	G2	M	81	Ex
27	T3b	G3	M	71	Ex
28	T1	G3	M	77	Ex
29	T1	G3	M	68	Ex
30	T3b	G3	M	68	Ex
31	T2a	G3	M	56	Ex
32	T2a	G2	M	75	No

All clinical specimens used for this study were selected from therapy- naïve patients.

Validated histological sections of non-neoplastic tissue were used, and the birefringence of the collagen was highlighted through the polarized light/dark microscope analysis (Fig. 1**A**). The anisotropy index of non-neoplastic lamina propria of the entire tissue section was measured using several regions of interest (ROIs) (44–120 ROIs according to the amount of tissue section), and each ROI with an area of 0.01 mm^2. Next, the anisotropy value of the same tissue section was calculated using half of the ROIs used for the entire section (Group 1), and the same procedure was repeated by selecting the other half of ROIs (Group 2) (Fig. 1**B**). Because the neoplastic tissue is more heterogeneous than the non-neoplastic tissue due to the presence of neoplastic niches, inflammatory infiltrate, and neo-vessels, we investigated if the same strategy could be adopted for measuring the anisotropy index of the neoplasia (Fig. 1**C**). We identified that the minimum number of ROIs representative of the anisotropy index of the entire tissue section was 22, corresponding to an area of 0.23 mm^2. Moreover, the same number of ROIs was applicable to both non-neoplastic (Fig. 1**D**) and neoplastic tissue (Fig. 1**E**).

Topographic reorganization of ECM is associated with bladder cancer stage and grade

After having standardized the methodology to perform the analysis, we investigated the association between the topography of collagen fibers of the lamina propria and the stage of bladder cancer. The anisotropy index was evaluated in the lamina propria of non-neoplastic, dysplastic, and neoplastic tissues (therapy-naïve NMIBC or MIBC, Table 1) by applying the validated 22 ROIs strategy and excluding areas enriched in blood vessels.

In the context of the neoplastic bladder, the non-neoplastic and dysplastic tissue showed similar anisotropy index and, therefore, were combined for the following analyses. Likewise, for the superficial tumors, such as Carcinoma *in situ* (Cis) and Ta, we did not find differences (data not shown), and the data were pooled together. We identified that each stage of the tumor had a higher anisotropy index than non-neoplastic/dysplastic tissues. The anisotropy index of the superficial tumors (Cis + Ta) was higher compared to the non-neoplastic/dysplastic tissues, and even greater in tumors breaking the basal lamina and invading the lamina propria (T1), while the anisotropy index was similar in T1 and muscle-invasive (i.e., >T1) tumors. (Fig. 1**F**). Furthermore, we established an association between the anisotropy index and the tumor grade, as the anisotropy index increased from the non-neoplastic/dysplastic tissues to grade 2 and even more in grade 3 (Fig. 1**G**).

Topographic ECM remodeling of lamina propria precedes the onset of bladder cancer

The study on clinical specimens highlighted tissue remodeling in the neoplastic environment associated with a process of inflammation; although very informative, the use of BCa patient samples provides a snapshot of the TME rearrangement once the tumor is present, but it does not provide information on whether the topographic ECM remodeling is a potential marker of tumor onset. Thus, we implemented a preclinical model of bladder cancer, in which the rats exposed to the bladder-specific carcinogen BBN develop all steps of carcinogenesis, from the inflammatory status to the onset of atypia of a non-univocal nature, dysplasia, tumor onset and invasion. We followed the BBN effect on the bladder at different time points using ultrasound imaging (Fig. 2**A)** and histological analysis **(**Fig. 2**B)**.

Similarly to what was carried out for human samples, we standardized the data acquisition for rat bladder anisotropy measurement. Because the rat bladder is smaller than the human bladder, we used smaller ROIs and we identified that averaging the anisotropy measurement from 20 ROIs covering a total area of 0,0047 mm^2 was representative of the anisotropy of the entire lamina propria. The anisotropy index increased during the inflammatory processes, from the acute

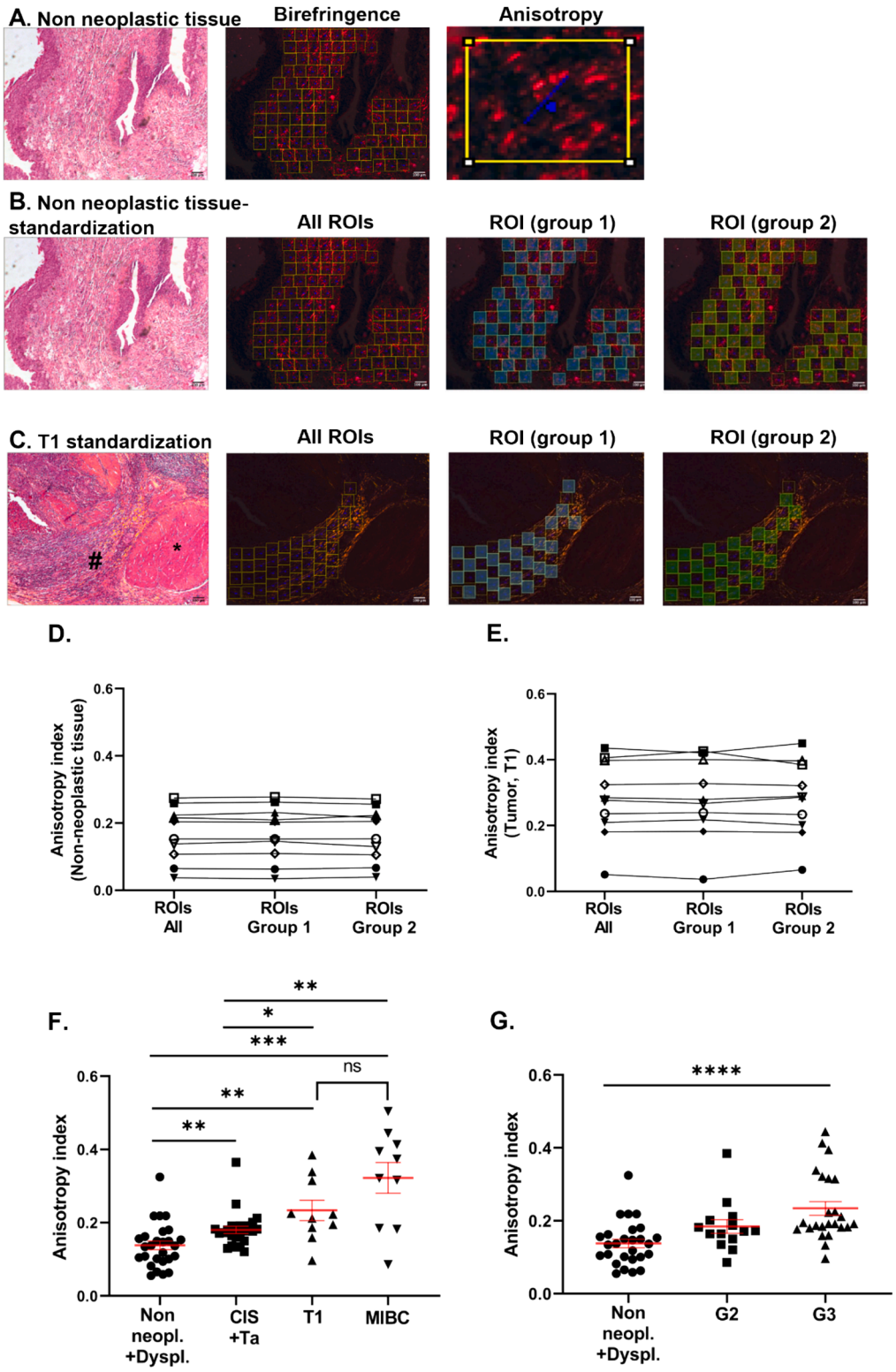

Fig. 1. Anisotropy of collagen fibrils in human bladder and urothelial cancers. A) Hematoxylin/eosin-stained sections of human bladder, followed by acquisition of collagen birefringence with polarized light/darkfield microscopy and analysis of the anisotropy (blue line that shows the average orientation of the fiber and the length that is proportional to the anisotropy index) in the region of interest (ROI). B) Standardization of the anisotropy measurement in the non-neoplastic and C) T1 bladder tumor (* shows muscle; # shows lamina propria of the bladder); each box in the darkfield microscopy represents a ROI with an area of 0.01 mm^2. D-E) Anisotropy index measurement in "all ROIs", "ROIs group 1" and "ROIs group 2" for ten patients, each represented by different symbol; paired Anova test did not show statistical difference among the three ways of measuring the anisotropy, both in the non-neoplastic or T1 tumor tissue. F) Anisotropy index according to the stage of the bladder cancer (non-neoplastic + dysplasia = 27 tissues; CIS + Ta = 24; T1 = 10; MIBC = 10). G) Anisotropy index according to the grade (non-neoplastic = 27; G2 = 14; G3 = 24) of the bladder cancer. Mean ± SEM are shown by red bars, and asterisks show the p value evaluated by means unpaired non-parametric two tail T-test (Mann-Whitney test) (*: $p < 0.05$; **: $p < 0.005$; ***: $p < 0.0005$; n.s.: not significant) and non-parametric ANOVA (Kruskal-Wallis test) (****: $p < 0.0001$). (For interpretation of the references to colour in this figure legend, the reader is referred to the web version of this article.)

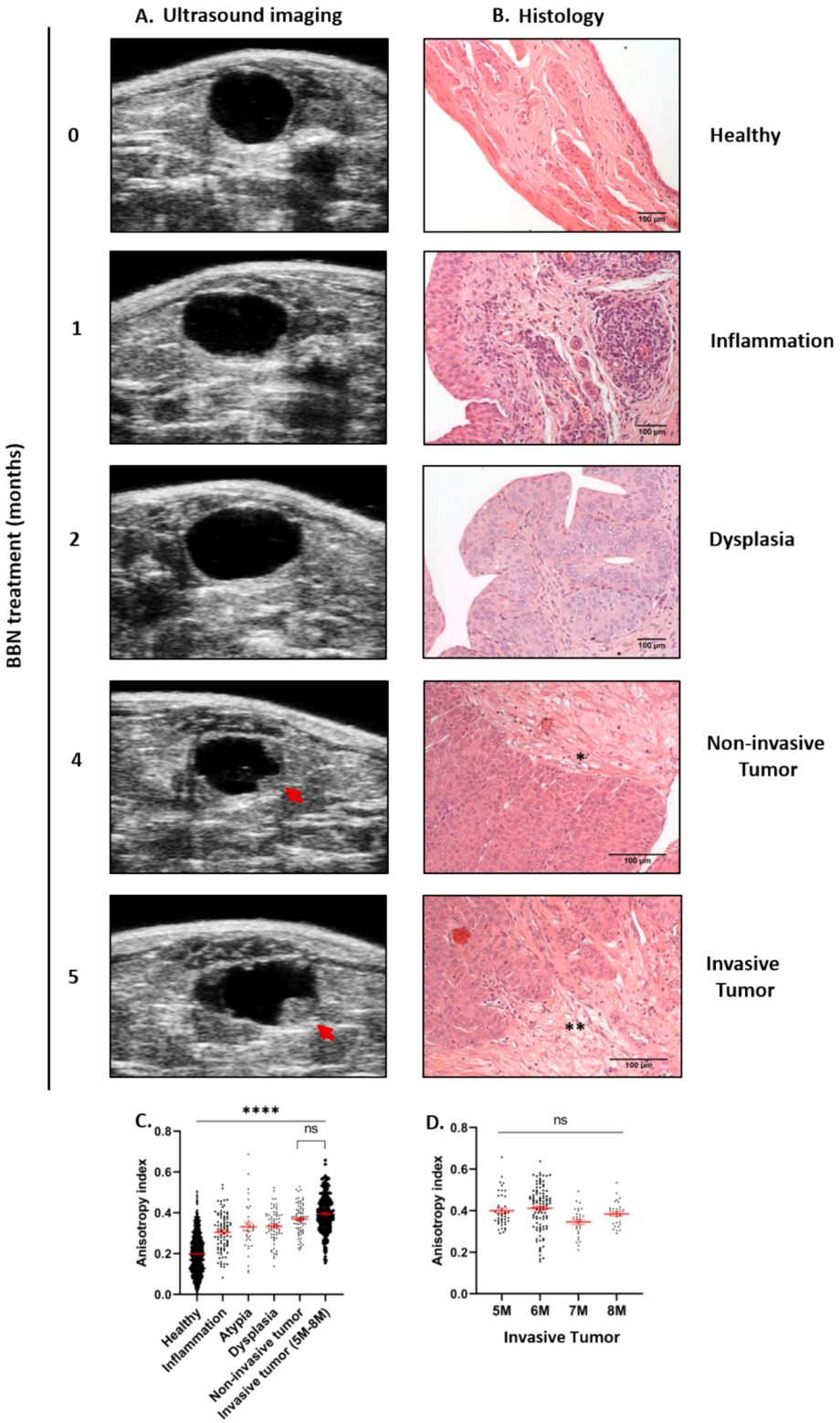

Fig. 2. Topographical modification of bladder lamina propria in the preclinical model of BBN-induced carcinogenesis. A) Follow-up of rat bladder modifications by ultrasound imaging during BBN treatment, from one animal representative of five with overlapping information. B) Histological section of rat bladder from untreated and BBN treated rats, showing acute inflammation that occurred at 2–4 weeks after treatment, dysplasia at 2 months of treatment, non-invasive tumor at 4 months after treatment and invasive T1 tumor after 5 months. C) Anisotropy index of collagen fibers in the rat bladder lamina propria in untreated (healthy) and BBN-treated rats at the different stages of tissue modification. D) Anisotropy index of collagen fibers in the rat bladder lamina propria with the presence of invasive T1 tumor for different months (5 months-8 months).

inflammation to atypia and dysplasia and further increased when the non-invasive tumor was present (Fig. 2**C**). The anisotropy index did not further increase when the tumor invaded the lamina propria at month 5 (Fig. 2**C**), even when the invasive T1 tumor remained in the lamina propria for several months, from month 5 to month 8 (Fig. 2**D**, **Supplementary Figure S1**).

In panel A red arrows indicate the visualization of the tumor in ultrasound acquisition. In panel B asterisks show the presence of tumor cells, and for the invasive T1 tumor rupture of the basal membrane separating the urothelium and lamina propria was also evident. In panels C and D, each symbol represents the value of the anisotropy index in a single ROI from at least 3 animals for each cohort or time point, for a total of 42 rats. Mean ± SEM are shown by red bars, and asterisks show the p-value evaluated by means non-parametric ANOVA (Kruskal-Wallis test) (****: $p < 0.0001$; n.s.: not significant).

ECM remodeling sets the ground for tumor growth, causing anticipation of tumor onset

To deepen the impact of ECM topography on the onset of the bladder tumor, we investigated the preclinical model of actinic cystitis, a pathological condition caused by pelvic radiotherapy in patients treated for prostate and rectum cancer [18,19]. Actinic cystitis is characterized by an accumulation of extracellular matrix proteins, in particular of collagen [19], resulting in tissue thickening and potentially in end-stage organ failure [7].In agreement with previous findings [20–23], a single session of X-ray irradiation (20 Gray) of the rat bladder (Fig. 3**A**) did not induce malignant transformation of the bladder, but four months later the bladder ECM was remodelled, and characterized by accumulation of collagen (Fig. 3**B**) and increased linearization of the collagen fibers (Fig. 3**C**). To establish the role of ECM topographic modification in setting the ground for tumor growth, we administered BBN via the drinking water after the induction of actinic cystitis (Fig. 4**A**). Four months after the X-ray irradiation, mice were treated with BBN, and once a week we monitored the onset and the growth of tumor by ultrasound imaging (Fig. 4**B-C**). In this setup we identified the presence of invasive T1 tumors after 3.5 months of BBN treatment (Fig. 4**D**), which represents an earlier time compared to treatment with the carcinogenic agent alone (Fig. 2).

Discussion

This study established the ultrastructural modification of the ECM in BCa, assessing the texture of collagen fibrils pattern of clinical and pre-clinical specimens. Using clinical and pre-clinical samples validated through histological examination, we identified that topographic modification of the extracellular microenvironment occurs during the inflammatory processes preceding and favoring the onset of bladder cancer. The implication of this study is the identification of a feature of the ECM that predicts the onset of bladder cancer, which can be deployed for the identification of patients and tissue areas at risk of tumor relapse.

To characterize the topographic remodeling of collagen fibers in bladder samples, we first established a standardized protocol to quantify the anisotropy index. The anisotropy index of collagen fibrils was evaluated in areas of the lamina propria, excluding the blood vessels, and it was established that measuring the anisotropy index in 0.23 mm^2 of the tissue section was the minimum area representative of the anisotropy observed throughout the entire lamina propria in the histological section. The progressive linearization of the texture of the collagen fibrils was associated with the steady increase of the stage of NMIBC, from the benign modification of the urothelium to the onset of superficial tumors Cis and Ta and the invasive T1 tumor, while for tumors that invaded the muscle layer the anisotropy index was similar to that of T1.

To deepen the associations reported in the clinical samples, which represent a snapshot of the clinical history of the disease, we used a preclinical model that allows monitoring the BCa onset and progression in eight months of treatment with the carcinogen BBN, from hyperplasia to papillary tumor, low- and high-grade carcinoma, non-invasive to invasive carcinoma [24]. The treatment induced a steady increase of the anisotropy index according to the progression of the inflammatory process, and further increased in the presence of the non-invasive tumor, as reported using clinical specimens. Invasion of the tumor started after five months of BBN treatment and did not further increase the linearization of collagen fibrils, which remained stable in the following four months of invasive neoplasia. The use of the preclinical model allowed us to appreciate the modification of the linearization of collagen fibrils that occurs during the inflammatory process and before the onset of the tumor, whose presence further increases the anisotropy of the lamina

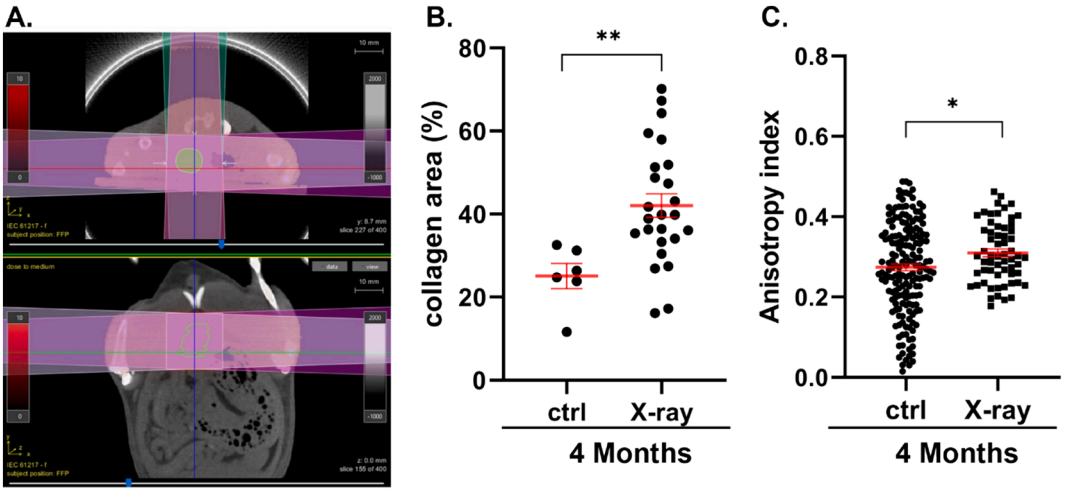

Fig. 3. ECM remodeling in preclinical model of actinic cystitis. A) Set up of X-ray irradiation, based on computerized tomography (CT) image of the rat bladder and the inclination of the three beams. B) The quantification of bladder area that expressed collagen in untreated (ctrl, control) and X ray-irradiated animals quantified in HE slides; each symbol represents the measurement in a tissue slice, with multiple slices measured for each bladder, in three animals. Mean ± SEM are shown by red bars and asterisks represent the p-values (unpaired non-parametric two-tail T-test, Mann-Whitney test). C) Anisotropy index of collagen fibers in the rat bladder lamina propria in untreated (ctrl, control) and X ray-irradiated rats; each symbol represents the value of anisotropy index in a single ROI; Mean ± SEM are shown by red bars and asterisks the p values (unpaired non-parametric two tail T-test, Mann-Whitney test) (*: $p < 0.05$; **: $p < 0.005$). (For interpretation of the references to colour in this figure legend, the reader is referred to the web version of this article.)

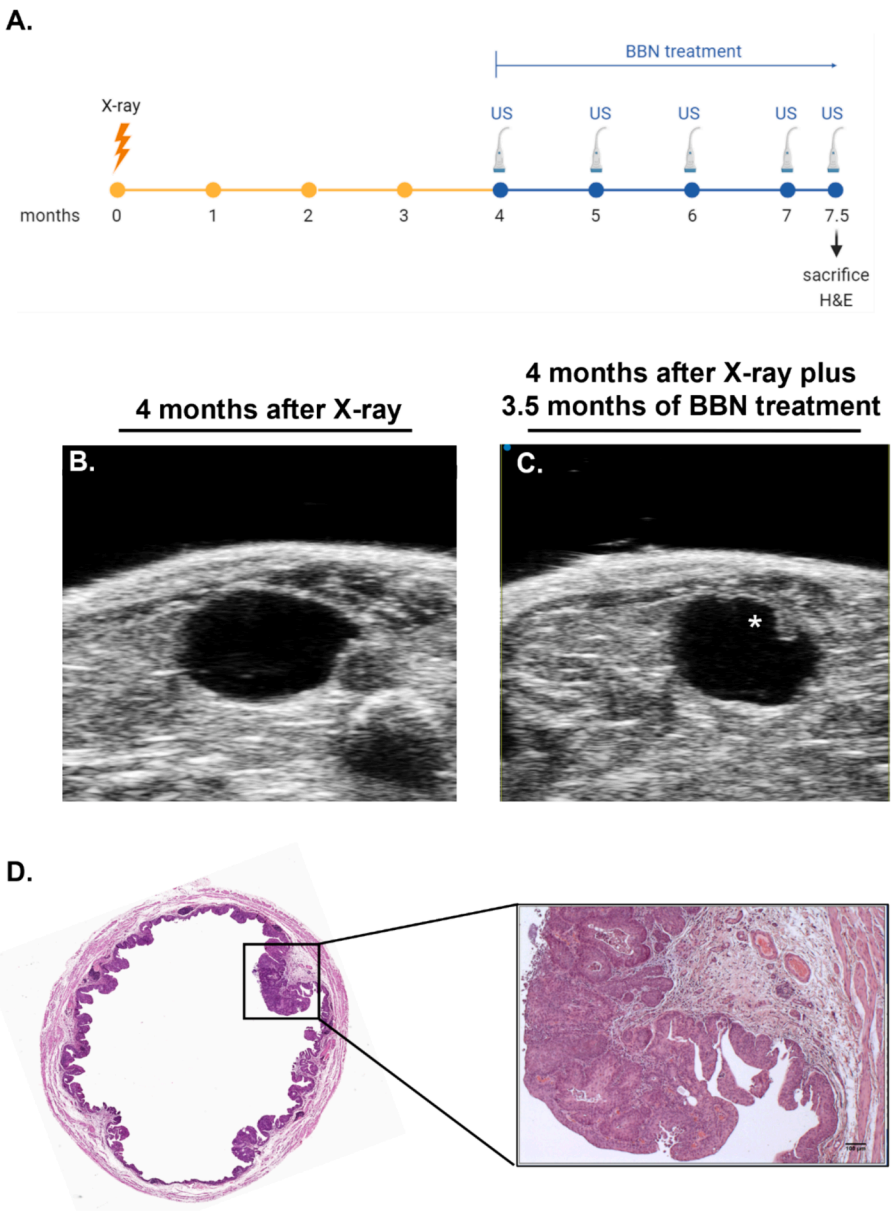

Fig. 4. Earlier onset of bladder tumor in remodeled ECM. A) Timeline of X-ray irradiation and BBN treatment. (US: ultrasound imaging). B) US imaging of rat bladder 4 months after X-ray irradiation. C) US imaging of rat bladder 4 months after X-ray treatment plus 3.5 months of BBN treatment. * Shows the presence of tumor. D) Histology of rat bladder 4 months after X-ray treatment plus 3.5 months of BBN treatment. The magnification shows the invasion of tumor cells inside the lamina propria. Panels B to D show information from one representative animal of three with overlapping information.

propria.

To assess the causative effect of collagen topography on tumor onset, we demonstrated that linearization of collagen fibrils induced by radiotherapy favors the development of the tumor, inducing a temporal advance in its development. This study identified that the topographic modification of the collagen fibrils of the bladder lamina propria precedes the onset and invasion of bladder cancer. Remodelling of the tumor microenvironment was associated with a reactive stroma representative of inflammatory process.

We recognize that linearization of collagen fibrils is one of the several modifications in the extracellular microenvironment that rise after radiotherapy and may not be the only manifestation associated with X-ray irradiation that promotes early tumor onset. Nonetheless, topographic modification of the extracellular microenvironment occurs during the inflammatory processes preceding the onset of the bladder cancer, and further remodelling of the topography of the ECM before the invasion is provided by the presence of the neoplastic cells. Modification of the ECM texture represents one of the events responsible for setting the neoplastic background also in primary bladder cancer, as proposed to explain the metastatic spread of the disease [25–27]. Sex-specific differences for BCa have been explained by differences in the urothelial TME, for instance in the local microbiome [28] and immune infiltration [29]. As a consequence, also the extent of the modification of the ECM topography must be investigated in male and female bladder cancer patients, which was not possible in this study due to the limited number of female patients.

In the context of the neoplastic environment, characterized by an inflammatory process, the topographic reconfiguration is a proxy of tissue transformation, and could represent a marker for the identification of the non-neoplastic tissue at risk of tumor relapse. This information paves the way for exploring the use of drugs inhibiting ECM-modifying enzymes, such as the lysyl oxidases (LOX) and LOX-like proteins (LOXL) [30–32], and to investigate the delivery as intravesical instillation to reduce their side effects [33].

Findings from this study are exploitable for setting the ground to identify patients and bladder areas at risk of tumor relapse, both i) *ex-vivo*, by assessing the anisotropy index of collagen fibers on non-neoplastic and suspicious H&E tissue sections collected during TURBT using polarized light microscopy or Brillouin microscopy [37], and ii) *in vivo*, by assessing the three-dimensional organization of collagen fibrils using innovative imaging-based techniques, such as elastography [34,35] ormultiparametric magnetic resonance imaging [36], and iii) for the delivery of novel adjuvant therapy targeting ECM remodelling in order to revert topographic modifications to a physiological low linearization of the collagen fibers, aiming to decrease the disease progression/relapse.

Experimental procedures

Human patient cohort

Seventy-one clinical specimens from 32 patients (29 men, 3 women) with a diagnosis of bladder cancer were used; clinical specimens were from 12 radical cystectomies and 20 transurethral resections of bladder tumors (TURBTs), in which both tumor and paired non-tumor areas were available for all patients (Table 1). All surgical specimens encompassed the entire bladder wall, and were staged according TNM classification [38] and morpho-architectural criteria according to WHO classification [39]. Formalin-fixed paraffin-embedded blocks were retrieved and stained using automatic Hematoxylin/Eosin (HE) slide stainer (HistoCore SPECTRA ST, Leica). The HE slides were reviewed by an expert genitourinary pathologist. The study was carried out in compliance with the principles of the Declaration of Helsinki; all patients signed an informed consent agreeing to deliver their own anonymous information for future studies. The study received approval from the Institutional Review Board.

Rat model of bladder carcinogenesis

Forty-two eight-week-old, 150–175 g female Fisher rats (Charles River, Germany) were housed in the animal facility at IRCCS San Raffaele Hospital under standard conditions (temperature: 22 ± 2 °C; humidity: 50 ± 10 %; light/dark cycle: 12-h light and 12-h dark). After a 1-week period of acclimatization, the rats were evenly divided into two groups: i) tumor, which was watered with 0.05 % N-(4-hydroxybutyl) nitrosamine (BBN; Sigma Aldrich) and ii) control, which was watered with normal drinking water. Animals were euthanized by CO_2, the bladder was filled with about 200 μl of formalin using a 22 G cannula (BD, Italy), placed in formalin for 24 h, and then embedded in paraffin.

Rat model of actinic cystitis

Three eight-week-old, 150–175 g female Fisher rats were housed as reported above, and after a 1-week period of acclimatization, the rat bladder was X-ray irradiated. Animals were anesthetized with isofluorane 2–4 %, and the bladder was filled with 450 μl of sterile saline solution using a PE50 catheter [40]. X-ray irradiation of the bladder was performed as reported [41]. All procedures and studies involving animals were performed under protocols approved by the IRCCS Ospedale San Raffaele Institutional Animal Care and Use Committee, and in accordance with national and international standard guidelines.

Ultrasound image analysis

Ultrasound (US) imaging was performed to monitor the presence of bladder transformation [42], using the Vevo3100 LAZR-X Imaging Station equipped with an MX250D transducer (FUJIFILM VisualSonics, Amsterdam, the Netherlands). The ultrasound signal of axial sections of the rat bladder was acquired using the following settings: frequency: 21 MHz; gain: 15 dB; step size: 200 μm. B-mode 3D ultrasound images of the rat bladder were acquired and analyzed with VevoLab 3.2.5 software.

Collagen birefringence and FibrilTool analysis

Collagen birefringence was acquired on the HE stained tissues by using the polarized light in darkfield microscope (Zeiss AxioImager M2M) and virtual images were generated with the use of Axio Vision Imaging software (AxioVision, vers. SE64 Rel.4.9.1). All images were captured using 5X objective (NEOFLUAR 5X- NA 0.15) and 10X objective (APOCHROMAT 10X – NA 0.45). Anisotropy was analyzed by using the ImageJ software plug-in FibrilTool [43]. The degree of collagen fibrils organization is expressed in a range from 0 to 1; 0 that represents random orientation of the fibrils, and 1 that is the maximum of linearization of collagen fibrils.

Collagen quantification

Collagen quantification from hematoxylin/eosin stained tissue slices was performed by quantifying collagen birefringence from images acquired with polarized light in dark field microscope (Zeiss AxioImager M2M). All images were captured using 10X objective (APOCHROMAT 10X – NA 0. 4 5) and analyzed with ImageJ software.

Statistical analysis

All experiments were repeated with at least three independent biological replicates. Mann-Whitney test and Kruskal-Wallis test were performed using GraphPad Prism v. 8. Data are shown as mean ± SEM.

CRediT authorship contribution statement

Chiara Venegoni: Writing – review & editing, Methodology, Investigation, Data curation. **Filippo Pederzoli:** Writing – review & editing, Investigation. **Irene Locatelli:** Writing – review & editing, Methodology, Investigation. **Elisa Alchera:** Methodology. **Laura Martinez-Vidal:** Writing – review & editing. **Alessia Di Coste:** Writing – review & editing. **Marco Bandini:** Writing – review & editing. **Andrea Necchi:** Data curation. **Francesco Montorsi:** Data curation. **Andrea Salonia:** Data curation. **Marco Moschini:** Writing – review & editing. **Jithin Jose:** Data curation. **Federico Scarfò:** Investigation. **Roberta Lucianò:** Investigation, Data curation. **Massimo Alfano:** Writing – original draft, Supervision, Funding acquisition, Data curation, Conceptualization.

Declaration of competing interest

The authors declare that they have no known competing financial interests or personal relationships that could have appeared to influence the work reported in this paper.

Data availability

Data will be made available on request.

Acknowledgments

This research was funded by the European Union's Horizon 2020 research and innovation program, under the Marie Skłodowska-Curie Action grant agreement No. 812772 (Phys2Biomed) and received funding from the European Union's Horizon 2020 research and innovation program under grant agreement No. 801126 (EDIT).

We thank Dr. Antonello Spinelli, Dr. Laura Perani, Dr. Amleto Fiocchi (Preclinical Imaging Facility, IRCCS Ospedale San Raffaele), and Dr. Cesare Covino (ALEMBIC Facility, IRCCS Ospedale San Raffaele) for their support.

Appendix A. Supplementary data

Supplementary data to this article can be found online at https://doi.org/10.1016/j.mbplus.2024.100154.

References

[1] E. Brett, M. Sauter, E. Timmins, O. Azimzadeh, M. Rosemann, J. Merl-Pham, et al., Oncogenic linear collagen VI of invasive breast cancer is induced by CCL5, J. Clin. Med. 9 (2020).

[2] S.Z. Despotovic, D.N. Milicevic, A.J. Krmpot, A.M. Pavlovic, V.D. Zivanovic, Z. Krivokapic, et al., Altered organization of collagen fibers in the uninvolved human colon mucosa 10 cm and 20 cm away from the malignant tumor, Sci. Rep. 10 (2020) 6359.

[3] M. Nebuloni, L. Albarello, A. Andolfo, C. Magagnotti, L. Genovese, I. Locatelli, et al., Insight on colorectal carcinoma infiltration by studying perilesional extracellular matrix, Sci. Rep. 6 (2016) 22522.

[4] D. Park, E. Wershof, S. Boeing, A. Labernadie, R.P. Jenkins, S. George, et al., Extracellular matrix anisotropy is determined by TFAP2C-dependent regulation of cell collisions, Nat. Mater. 19 (2020) 227–238.

[5] J.A. Pedersen, S. Lichter, M.A. Swartz, Cells in 3D matrices under interstitial flow: Effecs of extracellular matrix alignment on cell shear stress and drag forces, J. Biomech. 43 (2010) 900–905.

[6] A. Ray, O. Lee, Z. Win, R.M. Edwards, P.W. Alford, D.H. Kim, et al., Anisotropic forces from spatially constrained focal adhesions mediate contact guidance directed cell migration, Nat. Commun. 8 (2017) 14923.

[7] L. Martinez-Vidal, V. Murdica, C. Venegoni, F. Pederzoli, M. Bandini, A. Necchi, et al., Causal contributors to tissue stiffness and clinical relevance in urology, Commun. Biol. 4 (2021) 1011.

[8] J. Winkler, A. Abisoye-Ogunniyan, K.J. Metcalf, Z. Werb, Concepts of extracellular matrix remodelling in tumour progression and metastasis, Nat. Commun. 11 (2020) 5120.

[9] F. Pederzoli, M. Raffo, H. Pakula, F. Ravera, P.V. Nuzzo, M. Loda, Stromal cells in prostate cancer pathobiology: friends or foes? Br. J. Cancer 128 (2023) 930–939.

[10] V. Mohan, A. Das, I. Sagi, Emerging roles of ECM remodeling processes in cancer, Semin. Cancer Biol. 62 (2020) 192–200.

[11] I.M. Joshi, M. Mansouri, A. Ahmed, R.A. Simon, P.E. Bambizi, D.E. Desa, et al. **Microengineering 3D Collagen Matrices with Tumor-Mimetic Gradients in Fiber Alignment**. *bioRxiv* 2023.

[12] J.Y. Lichtenberg, E. Ramamurthy, A.D. Young, T.P. Redman, C.E. Leonard, S. K. Das, et al., Leader cells mechanically respond to aligned collagen architecture to direct collective migration, PLoS One 19 (2024) e0296153.

[13] M. Alfano, I. Locatelli, C. D'Arrigo, M. Mora, G. Vozzi, A. De Acutis, et al., Lysyl-oxidase dependent extracellular matrix stiffness in Hodgkin lymphomas: mechanical and topographical evidence, Cancers (Basel) 14 (2022).

[14] O. Nadiarnykh, R.B. LaComb, M.A. Brewer, P.J. Campagnola, Alterations of the extracellular matrix in ovarian cancer studied by Second Harmonic Generation imaging microscopy, BMC Cancer 10 (2010) 94.

[15] L. Genovese, L. Zawada, A. Tosoni, A. Ferri, P. Zerbi, R. Allevi, et al., Cellular localization, invasion, and turnover are differently influenced by healthy and tumor-derived extracellular matrix, Tissue Eng. A 20 (2014) 2005–2018.

[16] M. Alfano, M. Nebuloni, R. Allevi, P. Zerbi, E. Longhi, R. Luciano, et al., Linearized texture of three-dimensional extracellular matrix is mandatory for bladder cancer cell invasion, Sci. Rep. 6 (2016) 36128.

[17] R.T. Bryan, S.I. Collins, M.C. Daykin, M.P. Zeegers, K.K. Cheng, D.M. Wallace, et al., Mechanisms of recurrence of Ta/T1 bladder cancer, Ann. R. Coll. Surg. Engl. 92 (2010) 519–524.

[18] M.S. Mangano, A. De Gobbi, M. Ciaccia, C. Lamon, F. Beniamin, L. Maccatrozzo, Actinic cystitis: Causes, treatment and experience of a single centre in the last five years, Urologia 85 (2018) 25–28.

[19] B.M.M. Zwaans, K.A. Wegner, S.N. Bartolone, C.M. Vezina, M.B. Chancellor, L. E. Lamb, Radiation cystitis modeling: A comparative study of bladder fibrosis radio-sensitivity in C57BL/6, C3H, and BALB/c mice, Physiol. Rep. 8 (2020) e14377.

[20] B.R. Rajaganapathy, J.J. Janicki, P. Levanovich, P. Tyagi, J. Hafron, M. B. Chancellor, et al., Intravesical liposomal tacrolimus protects against radiation cystitis induced by 3-beam targeted bladder radiation, J. Urol. 194 (2015) 578–584.

[21] D. Giglio, C. Wasen, J. Molne, D. Suchy, J. Swanpalmer, J. Jabonero Valbuena, et al., Downregulation of toll-like receptor 4 and IL-6 following irradiation of the rat urinary bladder, Clin. Exp. Pharmacol. Physiol. 43 (2016) 698–705.

[22] R. Soler, A. Vianello, C. Fullhase, Z. Wang, A. Atala, S. Soker, et al., Vascular therapy for radiation cystitis, Neurourol. Urodyn. 30 (2011) 428–434.

[23] N. Oscarsson, L. Ny, J. Molne, F. Lind, S.E. Ricksten, H. Seeman-Lodding, et al., Hyperbaric oxygen treatment reverses radiation induced pro-fibrotic and oxidative stress responses in a rat model, Free Radic. Biol. Med. 103 (2017) 248–255.

[24] C. Vasconcelos-Nobrega, A. Colaco, C. Lopes, P.A. Oliveira, Review: BBN as an urothelial carcinogen, In Vivo 26 (2012) 727–739.

[25] M. Akhtar, A. Haider, S. Rashid, A. Al-Nabet, Paget's, "seed and soil" theory of cancer metastasis: An idea whose time has come, Adv. Anat. Pathol. 26 (2019) 69–74.

[26] I.J. Fidler, The pathogenesis of cancer metastasis: The 'seed and soil' hypothesis revisited, Nat. Rev. Cancer 3 (2003) 453–458.

[27] J. Mikula-Pietrasik, P. Uruski, A. Tykarski, K. Ksiazek, The peritoneal "soil" for a cancerous "seed": A comprehensive review of the pathogenesis of intraperitoneal cancer metastases, Cell. Mol. Life Sci. 75 (2018) 509–525.

[28] F. Pederzoli, R. Ferrarese, V. Amato, I. Locatelli, E. Alchera, R. Luciano, et al., Sex-specific alterations in the urinary and tissue microbiome in therapy-naive urothelial bladder cancer patients, Eur. Urol. Oncol. 3 (2020) 784–788.

[29] H.A. Abdel-Hafiz, S.K. Kailasam Mani, W. Huang, K.H. Gouin 3rd, Y. Chang, T. Xiao, et al., Single-cell profiling of murine bladder cancer identifies sex-specific transcriptional signatures with prognostic relevance, iScience 26 (2023) 107703.

[30] R.A. Kore, A.K. Bagchi, K.I. Varughese, J.L. Mehta, The structural basis of effective LOX-1 inhibition, Future Med. Chem. 14 (2022) 731–743.

[31] O. Saatci, A. Kaymak, U. Raza, P.G. Ersan, O. Akbulut, C.E. Banister, et al., Targeting lysyl oxidase (LOX) overcomes chemotherapy resistance in triple negative breast cancer, Nat. Commun. 11 (2020) 2416.

[32] N. Yang, D.F. Cao, X.X. Yin, H.H. Zhou, X.Y. Mao, Lysyl oxidases: Emerging biomarkers and therapeutic targets for various diseases, Biomed. Pharmacother. 131 (2020) 110791.

[33] A. Herchenhan, F. Uhlenbrock, P. Eliasson, M. Weis, D. Eyre, K.E. Kadler, et al., Lysyl oxidase activity is required for ordered collagen fibrillogenesis by tendon cells, J. Biol. Chem. 290 (2015) 16440–16450.

[34] X. Hu, C. Sun, X. Ren, S. Ge, C. Xie, X. Li, et al., Contrast-enhanced ultrasound combined with elastography for the evaluation of muscle-invasive bladder cancer in rats, J. Ultrasound Med. 42 (2023) 1999–2011.

[35] X.Z. Huang, A.Y. Zhou, M.W. Liu, Y. Zhang, P. Xu, Shear wave elasticity differentiation between low- and high-grade bladder urothelial carcinoma and correlation with collagen fiber content, J. Ultrasound Med. 40 (2021) 113–122.

[36] R.T. Abouelkheir, A. Abdelhamid, M. Abou El-Ghar, T. El-Diasty, Imaging of bladder cancer: standard applications and future trends, Medicina (Kaunas) 57 (2021).

[37] L. Martinez-Vidal, C. Testi, E. Pontecorvo, F. Pederzoli, E. Alchera, I. Locatelli, et al., Progressive alteration of murine bladder elasticity in actinic cystitis detected by Brillouin microscopy, Sci. Rep. 14 (2024) 484.

[38] M.J. Magers, A. Lopez-Beltran, R. Montironi, S.R. Williamson, H.Z. Kaimakliotis, L. Cheng, Staging of bladder cancer, Histopathology 74 (2019) 112–134.

[39] Tateo, V., Mollica, V., Rizzo, A., Santoni, M., Massari, F. (2023). Re: WHO Classification of Tumours, 5th Edition, Volume 8: Urinary and Male Genital Tumours. *Eur. Urol.*; 84: 348-349.

[40] C. Brown, Urethral catheterization of the female rat, Lab Anim. (NY) 40 (2011) 111–112.

[41] L. Martinez-Vidal, M. Chighizola, M. Berardi, E. Alchera, I. Locatelli, F. Pederzoli, et al., Micro-mechanical fingerprints of the rat bladder change in actinic cystitis and tumor presence, Commun. Biol. 6 (2023) 217.

[42] E. Alchera, M. Monieri, M. Maturi, I. Locatelli, E. Locatelli, S. Tortorella, et al., Early diagnosis of bladder cancer by photoacoustic imaging of tumor-targeted gold nanorods, Photoacoustics 28 (2022) 100400.

[43] A. Boudaoud, A. Burian, D. Borowska-Wykret, M. Uyttewaal, R. Wrzalik, D. Kwiatkowska, et al., FibrilTool, an ImageJ plug-in to quantify fibrillar structures in raw microscopy images, Nat. Protoc. 9 (2014) 457–463.